Research Square

Preprints are preliminary reports that have not undergone peer review.
They should not be considered conclusive, used to inform clinical practice,
or referenced by the media as validated information.

Integrated transcriptomic and metabolomic analyses reveal developmental and metabolic differences between wild and cultivated Cordyceps chanhua

Wei Ji
Lianyungang Academy of Agricultural Sciences
Xiaomei Liu
Lianyungang Academy of Agricultural Sciences
Xueyan Tang
Lianyungang Academy of Agricultural Sciences
Jintao Ge
lygnkygjt@126.com

Lianyungang Academy of Agricultural Sciences
Wenying Su
Lianyungang Academy of Agricultural Sciences
Wenbo Chai
Lianyungang Academy of Agricultural Sciences
Lijuan Hou
Jiangsu Academy of Agricultural Sciences
Fuhou Li
Jiangsu Ocean University

Research Article

Keywords: Cordyceps chanhua, transcriptomics, untargeted metabolomics, fruiting body development, functional food ingredients

Posted Date: June 12th, 2026

DOI: https://doi.org/10.21203/rs.3.rs-9879572/v1

License: This work is licensed under a Creative Commons Attribution 4.0 International License.
Read Full License

Additional Declarations: No competing interests reported.

Abstract

Cordyceps chanhua is an entomopathogenic fungus with both edible and medicinal value. However, the molecular differences between wild and cultivated *C. chanhua* during developmental differentiation and functional component accumulation remain poorly understood. In this study, transcriptome sequencing, untargeted metabolomics, and integrated transcriptome–metabolome analysis were used to compare cultivated fruiting bodies and mycelia (AF and AM) with wild fruiting bodies and mycelia (WF and WM), with a focus on gene expression, metabolic reprogramming, and bioactive nucleoside accumulation during the transition from mycelia to fruiting bodies. A total of 1,000 differentially expressed genes and 370 differentially accumulated metabolites were identified in AF vs AM, whereas 1,080 differentially expressed genes and 602 differentially accumulated metabolites were detected in WF vs WM, indicating extensive transcriptional and metabolic remodeling during developmental transition. In cultivated samples, the differential metabolites were mainly associated with amino acid metabolism, membrane lipid remodeling, and secondary metabolism. In contrast, those in wild samples were more closely related to glutathione metabolism, central carbon metabolism, and redox regulation. Integrated transcriptome–metabolome analysis further showed stronger correlations between differentially expressed genes and metabolites in cultivated samples, forming relatively compact functional modules. By contrast, wild samples exhibited a more dispersed gene–metabolite association pattern, suggesting distinct developmental and metabolic regulatory features under different growth environments. Functional component analysis showed that N_6-(2-hydroxyethyl)adenosine (HEA) was significantly enriched in mycelia, whereas adenosine accumulated preferentially in cultivated fruiting bodies, indicating stage-dependent accumulation of bioactive nucleosides. Overall, this study reveals developmental differentiation, metabolic reprogramming, and bioactive nucleoside accumulation differences between wild and cultivated *C. chanhua*. These findings provide multi-omics evidence for understanding quality formation in *C. chanhua*, optimizing cultivation conditions, and developing high-quality functional food ingredients.

Introduction

Cordyceps chanhua is an entomopathogenic fungus with both edible and medicinal value. It has a long history of use in China and represents an important resource among cordycipitoid fungi for food and functional product development (Zhu et al., 2023; Cai et al., 2024; Cai et al., 2025; Ji et al., 2025). In 2021, the fruiting body of *C. chanhua* was approved as a “new food raw material” by the National Health Commission of China, further promoting its application in functional foods and industrial production (Ji et al., 2024). Previous studies have shown that *C. chanhua* is rich in bioactive compounds, including nucleosides, polysaccharides, sterols, amino acids, and various secondary metabolites (Li et al., 2021; Di et al., 2023; Cao et al., 2024). These compounds have been associated with immunomodulatory, anti-inflammatory, antitumor, antimicrobial, and lipid metabolism-regulating activities (Lee et al., 2022; Wang et al., 2023; Wan et al., 2023; Zheng et al., 2024). With the increasing demand for natural bioactive

compounds and health-promoting foods, *C. chanhua* has considerable potential for the development of functional foods, nutraceuticals, and related products (Nxumalo et al., 2020; Dong et al., 2024).

At present, *C. chanhua* resources are mainly obtained from wild collection and artificial cultivation. Wild *C. chanhua* develops under complex natural conditions, and its growth is influenced by multiple factors, including host insects, microhabitat conditions, nutrient availability, and environmental stress. As a result, wild samples often exhibit complex metabolic characteristics and ecological adaptability (Li et al., 2006; He et al., 2019; Hsu et al., 2025). However, wild resources are constrained by host distribution, habitat conditions, and collection intensity, making it difficult to meet the demand for stable and large-scale utilization. In contrast, artificial cultivation provides a feasible approach for the sustainable supply and quality control of *C. chanhua*. Nevertheless, differences in culture substrates, growth environments, and developmental conditions may lead to variations in metabolic composition, nucleoside accumulation, and certain biological functions between cultivated and wild samples (Li et al., 2006). Therefore, clarifying the molecular differences between wild and cultivated *C. chanhua* during developmental differentiation and bioactive compound formation is essential for understanding its quality formation and optimizing cultivation strategies.

The transition from mycelia to fruiting bodies is a key developmental process in the fungal life cycle. It involves the shift from vegetative growth to reproductive development and is accompanied by changes in energy metabolism, amino acid metabolism, nucleoside metabolism, membrane lipid remodeling, and secondary metabolism. With advances in high-throughput sequencing and metabolomics, multi-omics integration has become an effective approach for elucidating fungal developmental differentiation and metabolic regulation (Yin et al., 2012; Ding, 2021; Thananusak et al., 2023). Transcriptomics captures dynamic changes in gene expression, whereas metabolomics reflects downstream metabolic responses. Their integration provides a continuous view from gene regulation to metabolic phenotype, thereby helping to uncover the molecular basis of biological processes (Siddiqui, 2018; He et al., 2023). In related entomopathogenic fungi, such as *Cordyceps militaris*, previous studies have shown marked transcriptional differences between mycelial and fruiting body stages. The differentially expressed genes are mainly involved in amino acid metabolism, carbohydrate metabolism, lipid metabolism, nucleotide and nucleic acid metabolism, cordycepin biosynthesis, and secondary metabolism, and are subject to stage-specific transcriptional regulation (Yin et al., 2012; Yang et al., 2016; Thananusak et al., 2023). However, the coordinated transcriptomic and metabolic changes in wild and cultivated *C. chanhua* remain poorly characterized, particularly with respect to the reconstruction of key metabolic modules and their potential regulatory nodes during different developmental stages.

In this study, transcriptome sequencing and untargeted metabolomics were integrated to systematically compare gene expression patterns, metabolite profiles, and functional component accumulation in wild and cultivated *C. chanhua* at the mycelial and fruiting body stages. We focused on identifying differentially expressed genes, differentially accumulated metabolites, key metabolic pathways, and transcriptome–metabolome association networks during developmental transition in samples from different sources. This study aimed to reveal the molecular differences underlying developmental

differentiation and metabolic reprogramming between wild and cultivated *C. chanhua*, and to provide a theoretical basis for cultivation optimization, high-quality product development, and targeted regulation of bioactive compounds.

Materials and methods

Experimental materials

The experimental materials included artificially cultivated fruiting bodies and mycelia of *Cordyceps chanhua* provided by the Lianyungang Academy of Agricultural Sciences, which were designated as AF and AM, respectively. The cultivated fruiting bodies were collected on day 18 after artificial inoculation, when the fruiting bodies reached a length of approximately 6–8 cm. Wild fruiting bodies and mycelia of *C. chanhua* were collected from Yixing, Wuxi, Jiangsu Province, China, and were designated as WF and WM, respectively. All wild samples were collected before visible senescence.

Untargeted metabolomic analysis

Sample extraction

Samples were slowly thawed at 4°C, and 50–100 mg of each sample was accurately weighed into a centrifuge tube. Subsequently, 1 mL of extraction solvent [water/acetonitrile/isopropanol, 1:1:1, v/v/v] was added. The mixture was vortexed for 60 s and subjected to ultrasonic extraction at low temperature for 30 min. The extract was centrifuged at 12,000 rpm for 10 min at 4°C, and the supernatant was collected and incubated at − 20°C for 1 h to precipitate proteins. After a second centrifugation at 12,000 rpm for 10 min at 4°C, the supernatant was collected and vacuum-dried. The dried residue was reconstituted in 200 µL of 50% acetonitrile, vortexed thoroughly, and centrifuged at 14,000 rpm for 15 min at 4°C. The resulting supernatant was used for LC–MS analysis (Ghirardo et al., 2020).

Liquid chromatography and mass spectrometry conditions

Metabolomic data were acquired using an ultra-high-performance liquid chromatography system (Vanquish UPLC, Thermo Fisher Scientific, USA) coupled with a high-resolution mass spectrometer (Q Exactive HFX, Thermo Fisher Scientific, USA).

Chromatographic separation was performed on a Waters HSS T3 column (100 mm × 2.1 mm, 1.8 µm). Mobile phase A consisted of ultrapure water containing 0.1% formic acid, and mobile phase B consisted of acetonitrile containing 0.1% formic acid. The flow rate was 0.3 mL/min, the column temperature was maintained at 40°C, and the injection volume was 2 µL. The gradient elution program was as follows: 0–1 min, 100% A; 1–12 min, 100% A to 5% A; 12–13 min, 5% A; 13–13.1 min, 5% A to 100% A; and 13.1–17 min, 100% A. During analysis, all samples were kept in the autosampler at 4°C. To minimize the influence

of instrumental signal drift, samples were analyzed in a randomized order, and quality control (QC) samples were inserted at regular intervals throughout the analytical sequence to monitor system stability and data reliability.

For mass spectrometry, both MS1 and MS2 data were acquired using an electrospray ionization (ESI) source. The sheath gas flow rate was set to 40 arbitrary units, and the auxiliary gas flow rate was set to 10 arbitrary units. The spray voltage was + 3000 V in positive ion mode and − 2800 V in negative ion mode. The ion source temperature was 350°C, and the ion transfer tube temperature was 320°C. Data were acquired in Full MS-ddMS2 mode under both positive and negative ionization modes. The MS1 scan range was m/z 70–1050, with a resolution of 70,000 for MS1 and 17,500 for MS2.

Metabolomic data preprocessing and metabolite identification

Raw mass spectrometry data were preprocessed using Progenesis QI software (Waters Corporation, Milford, USA). The preprocessing steps included baseline correction, peak detection, peak matching, retention time correction, and peak alignment, resulting in a data matrix containing retention time, mass-to-charge ratio, and peak intensity information. Metabolites were subsequently identified by matching MS/MS spectra against an in-house traditional Chinese medicine MS/MS database developed by Sanshu Bio, together with corresponding fragmentation patterns. The reliability of metabolite identification was evaluated mainly according to the MS/MS fragment matching score. The score ranged from 0 to 1, with higher values indicating greater confidence in identification. In general, metabolite annotations with a score > 0.5 were considered to have relatively high confidence.

Determination of bioactive compounds

Determination of adenosine content

Approximately 1.000 g of *C. chanhua* fruiting body powder was accurately weighed and transferred into a 50 mL volumetric flask. About 45 mL of extraction solvent was added, followed by ultrasonic extraction for 80 min. After extraction, the solution was brought to volume with the extraction solvent and mixed thoroughly. The extract was centrifuged at 3,000 rpm for 3 min, and the supernatant was sequentially filtered through 0.45 μm and 0.22 μm membranes before liquid chromatographic analysis. The reference chromatographic conditions were as follows: C18 column (4.60 mm × 250 mm, 5 μm); column temperature, room temperature; UV detection wavelength, 254 nm; mobile phase, methanol/0.01 mol/L potassium dihydrogen phosphate solution (10:90, v/v); flow rate, 1.000 mL/min; injection volume, 20 μL. Adenosine content was quantified by comparing the peak area of the sample with that of the standard. Each assay was performed in triplicate.

Determination of N-(2-hydroxyethyl)adenosine content

Approximately 0.2000 g of *C. chanhua* powder was accurately weighed into a 20 mL stoppered test tube. Then, 10.0 mL of 10% aqueous methanol was added, followed by ultrasonic extraction for 30 min. The extract was filtered through a 0.22 μm membrane before liquid chromatographic analysis. The chromatographic conditions were as follows: C18 column (4.6 mm × 150 mm, 5 μm); column temperature, 35°C; detection wavelength, 268 nm; mobile phase, acetonitrile/0.01 mol/L potassium dihydrogen phosphate solution (10:90, v/v); flow rate, 1.000 mL/min; injection volume, 10 μL. N_6-(2-hydroxyethyl)adenosine (HEA) content was quantified by comparing the sample peak area with that of the standard. Each assay was performed in triplicate.

Transcriptome sequencing and analysis

Total RNA extraction and quality assessment

To ensure RNA quality and minimize degradation, sample handling was performed under strictly controlled conditions. Total RNA was extracted from tissue samples using appropriate extraction reagents and protocols according to the characteristics of the samples. RNA concentration and purity were determined using a NanoDrop 2000 spectrophotometer, and RNA integrity was assessed by agarose gel electrophoresis. Only RNA samples that passed quality control were used for subsequent library construction.

mRNA enrichment and fragmentation

Because eukaryotic mRNA generally contains a poly(A) tail at the 3' end, mRNA was enriched from total RNA using Oligo(dT)-conjugated magnetic beads based on complementary base pairing. The enriched mRNA was then fragmented using fragmentation buffer to generate short fragments suitable for library construction and next-generation sequencing.

cDNA library construction

Fragmented mRNA was used as the template for first-strand cDNA synthesis with random hexamer primers and reverse transcriptase. Second-strand cDNA was subsequently synthesized using buffer, dNTPs, and DNA polymerase I. The resulting double-stranded cDNA was purified using AMPure XP beads. After purification, end repair was performed to generate blunt ends, followed by the addition of an adenine residue at the 3' end to facilitate ligation with Y-shaped sequencing adapters.

Library amplification and sequencing

After library construction, PCR enrichment was performed for 15 cycles. The amplified products were separated by 2% agarose gel electrophoresis, and fragments of the expected size were recovered. The libraries were quantified using TBS380 with PicoGreen. Qualified libraries were pooled according to the required proportions and subjected to bridge PCR amplification on a cBot platform to generate clusters. Paired-end sequencing was then performed on a next-generation sequencing platform with a read length of 2 × 150 bp.

Transcriptome bioinformatic analysis

Raw reads generated from the sequencing platform were processed by removing adapter sequences, low-quality reads, and other contaminating sequences to obtain high-quality clean reads. All subsequent analyses were performed based on these clean reads. Transcriptome analysis mainly included sequencing data quality control, read alignment, and downstream transcriptomic analysis. Quality control involved read filtering, sequencing quality assessment, and sequence length distribution analysis. For alignment analysis, reads mapped to the reference genome were classified and quantified according to genome annotation information. Downstream transcriptomic analysis included differential expression analysis, alternative splicing analysis, novel transcript prediction, and sequence variation analysis.

Integrated transcriptome–metabolome analysis

Based on KEGG pathway annotations, differentially expressed genes and differentially accumulated metabolites associated with growth, development, and bioactive compound biosynthesis were selected for integrated analysis (Kanehisa & Goto, 2000; Kanehisa et al., 2025). Pearson correlation analysis was used to evaluate associations between gene expression levels and metabolite abundances, and correlations with $|r| > 0.8$ and $P < 0.05$ were considered significant. Gene–metabolite correlation networks and clustered heatmaps were subsequently constructed to identify coordinated relationships between key genes and metabolites during growth, development, and bioactive compound accumulation in *C. chanhua* (Siddiqui et al., 2018).

Results

Metabolomic quality control and multivariate statistical analysis

In positive ion mode, the total ion chromatograms (TICs) of the quality control (QC) samples showed high consistency in peak shape, peak intensity, and retention time (Fig. 1A), indicating good repeatability of the sample extraction procedure and stability of the LC–MS system. Principal component analysis (PCA) showed that the first two principal components, PC1 and PC2, explained 39.3% and 19.5% of the total variance, respectively. The QC samples were tightly clustered in the PCA score plot (Fig. 1B), further confirming the reliability of the metabolomic dataset and the stability of the instrumental analysis.

Sample similarity analysis based on Euclidean distance revealed clear metabolic differences among samples from different sources and tissue types (Fig. 1C). The metabolic profiles of cultivated fruiting bodies and mycelia were relatively similar, whereas wild fruiting bodies and mycelia showed lower similarity, suggesting stronger metabolic differentiation between developmental stages in wild *C. chanhua*.

Chemical classification of the identified metabolites showed that the major classes included carboxylic acids and derivatives (28.43%), fatty acyls (12.61%), prenol lipids (11.56%), organooxygen compounds (7.75%), steroids and steroid derivatives (6.83%), and glycerophospholipids (3.87%) (Fig. 1D). Other classes, including benzene derivatives (2.50%), flavonoids (1.84%), phenols (1.58%), organonitrogen compounds (1.51%), purine nucleosides (1.44%), indole derivatives (1.31%), pyridine derivatives (1.18%), coumarins (1.05%), and hydroxy acids (0.92%), accounted for smaller proportions. The remaining metabolites were assigned to the “Others” category, representing 15.63% of the total. Overall, the metabolite profile of *C. chanhua* was chemically diverse, with organic acids and derivatives, fatty acyls, and prenol lipids as the predominant metabolite classes.

Screening of differential metabolites

Based on Chemical Taxonomy annotations, the chemical classification of differential metabolites in each comparison group was analyzed (Fig. 2A). In the AF vs AM comparison, the differential metabolites were mainly assigned to glycerophospholipids (42.42%), fatty acyls (24.24%), and carboxylic acids and derivatives (18.18%), followed by prenol lipids (9.09%), whereas (5'→5')-dinucleotides and organooxygen compounds accounted for smaller proportions (3.03% each). In the WF vs WM comparison, the differential metabolites were predominantly classified as carboxylic acids and derivatives (36.17%), followed by fatty acyls (12.77%), prenol lipids (10.64%), glycerophospholipids (8.51%), and indoles and derivatives (8.51%). Other categories, including benzene and substituted derivatives, pteridines and derivatives, 5'-deoxyribonucleosides, hydroxy acids and derivatives, organonitrogen compounds, piperidines, pyrans, pyridines and derivatives, and pyrrolidines, accounted for relatively small proportions, each not exceeding 4.26%.

In the AF vs WF comparison, the differential metabolites were mainly distributed among glycerophospholipids (17.39%), carboxylic acids and derivatives (15.22%), and organooxygen compounds (15.22%), followed by fatty acyls (8.70%), indoles and derivatives (6.52%), and prenol lipids (6.52%). The remaining categories, including benzene and substituted derivatives, pteridines and derivatives, purine nucleotides, pyridines and derivatives, (5'→5')-dinucleotides, organonitrogen compounds, purine nucleosides, pyrans, pyrimidine nucleosides, and others, each accounted for a relatively low proportion (≤ 4.35%). In the AM vs WM comparison, the differential metabolites were mainly assigned to carboxylic acids and derivatives (25.71%), glycerophospholipids (21.43%), and fatty acyls (11.43%), followed by organooxygen compounds and prenol lipids (8.57% each), whereas the other categories represented smaller proportions.

Hierarchical clustering based on the relative abundances of differential metabolites showed that AF and AM clustered together, while WF and WM also showed relatively high similarity (Fig. 2B). This result indicates that samples from the same source shared more similar overall metabolic patterns, although clear metabolic differentiation was still observed between developmental stages.

Volcano plot analysis showed that a large number of differential metabolites were detected in each comparison group (Fig. 2C). In the AF vs AM comparison, 370 differential metabolites were identified, including 196 upregulated and 174 downregulated metabolites. In the AF vs WF comparison, 423 metabolites were upregulated and 184 were downregulated. In the AM vs WM comparison, 721 metabolites were upregulated and 353 were downregulated. In the WF vs WM comparison, 327 metabolites were upregulated and 275 were downregulated. These results indicate extensive metabolic differences among samples from different sources and developmental stages, with the most pronounced differences observed between mycelial samples.

UpSet analysis further revealed the shared and specific differential metabolites among the comparison groups (Fig. 2D). The AF vs AM comparison contained 53 shared and 5 specific differential metabolites; the AF vs WF comparison contained 75 shared and 5 specific differential metabolites; the AM vs WM comparison contained 112 shared and 8 specific differential metabolites; and the WF vs WM comparison contained 78 shared and 2 specific differential metabolites.

Venn diagram analysis showed that 12 differential metabolites were shared between the AF vs AM and WF vs WM comparisons (Fig. 2E). In addition, 57 metabolites were specific to AF vs AM, whereas 80 metabolites were specific to WF vs WM, indicating distinct metabolic remodeling patterns during the transition from mycelia to fruiting bodies in cultivated and wild *C. chanhua*.

Taken together, the chemical classification, multivariate clustering, and shared/specific metabolite analyses showed that both AF vs AM and WF vs WM exhibited clear stage-dependent metabolic differentiation and strong biological comparability. Therefore, subsequent pathway enrichment analysis and integrated transcriptome–metabolome analysis focused mainly on these two comparisons to reduce the confounding effects caused by the simultaneous overlap of source differences and developmental stage differences, thereby improving the interpretability of the results.

Differential metabolites and pathway enrichment analysis

To characterize the metabolic differences between cultivated fruiting bodies (AF) and mycelia (AM) of *Cordyceps chanhua*, differential metabolites were screened based on fold change and statistical significance. Figure 3A shows the $\log_2$ fold-change distribution of the major differential metabolites in AF relative to AM. Several metabolites were significantly upregulated in AF, including lactaroviolin, lacinilene C, doxorubicinol aglycone-3,4,5-trihydroxy, ganosporeric acid A, cGMP (guanosine 3',5'-cyclic monophosphate), absintholide, and thalictroidine. These metabolites are mainly related to alkaloids, nucleosides, and phenolic derivatives, suggesting marked changes in the accumulation of certain secondary metabolism-related compounds during fruiting body formation. In contrast, several metabolites were downregulated in AF, including norleucine, L-glutamic acid 5-phosphate, adenylosuccinate, propionylcarnitine, and various fatty acids and their derivatives, indicating that the transition from mycelia to fruiting bodies was accompanied by substantial changes in metabolites associated with primary metabolism.

KEGG pathway enrichment analysis was performed for the differential metabolites in AF vs AM, and pathway significance was evaluated using Fisher's exact test (Fig. 3B). Several pathways were significantly enriched ($P < 0.05$), including nicotine addiction, cocaine addiction, long-term potentiation, and olfactory transduction. It should be noted that these pathway names are derived from the KEGG annotation system and mainly reflect the assignment of related metabolites to signaling or receptor-associated annotation modules; they do not imply that *C. chanhua* possesses corresponding animal nervous system functions. In addition, pathways such as protein digestion and absorption and proximal tubule bicarbonate reclamation were also significantly enriched, suggesting broad metabolic remodeling during cultivated fruiting body formation.

To further compare metabolic differences between wild fruiting bodies (WF) and mycelia (WM), differential metabolites were screened using the same criteria (Fig. 3C). The number of upregulated metabolites in WF was higher than that of downregulated metabolites, and the overall magnitude of change was relatively large. The significantly upregulated metabolites included L-beta-aspartyl-L-phenylalanine, 5-aminopentanoate, lacinilene C, lactaroviolin, 5'-methylthioadenosine, betaine, carnitine, flavin mononucleotide (FMN), and oxidized glutathione. These metabolites are mainly associated with amino acid derivatives, peptides, and phenolic compounds, indicating enhanced accumulation of metabolites related to amino acid transformation, redox regulation, and specialized metabolism in wild fruiting bodies. By contrast, fewer metabolites were downregulated, mainly including several nucleosides, short peptides, and alkaloids, indicating that wild *C. chanhua* also underwent pronounced metabolic changes during fruiting body formation.

KEGG pathway enrichment analysis of the differential metabolites in WF vs WM showed that several pathways were significantly enriched ($P < 0.05$), including protein digestion and absorption, central carbon metabolism in cancer, thyroid hormone synthesis, and chlorocyclohexane and chlorobenzene degradation (Fig. 3D). Among these, enrichment of the central carbon metabolism in cancer pathway mainly reflected changes in metabolites associated with core carbon metabolism, such as glycolysis and the tricarboxylic acid cycle. Meanwhile, phenylalanine metabolism, glycine, serine and threonine metabolism, cysteine and methionine metabolism, and monobactam biosynthesis were also significantly enriched. In addition, enrichment of glutathione metabolism indicated marked changes in antioxidant-related metabolic processes during the wild fruiting body stage. Overall, the enriched pathways in WF vs WM were mainly associated with amino acid metabolism, central carbon metabolism, and stress-response-related processes, providing a basis for subsequent multi-omics integration.

To compare the accumulation of functional components across developmental stages and sample sources, the contents of N_6-(2-hydroxyethyl)adenosine (HEA) and adenosine were determined (Fig. 3E–H). HEA content was significantly higher in mycelia than in fruiting bodies. Under cultivated conditions, HEA content in AM was 0.83 ± 0.08%, significantly higher than that in AF (0.51 ± 0.08%; $P < 0.01$). Under wild conditions, HEA content in WM was 0.76 ± 0.05%, also significantly higher than that in WF (0.49 ± 0.08%; $P < 0.01$). Overall, HEA was enriched in mycelia under both cultivated and wild conditions and decreased during fruiting body formation. In contrast, adenosine exhibited different accumulation

patterns between cultivated and wild samples. Under cultivated conditions, adenosine content in AF was 1.47 ± 0.15%, significantly higher than that in AM (0.84 ± 0.12%; $P < 0.01$), indicating pronounced adenosine accumulation during the fruiting body stage. Under wild conditions, adenosine content in WF was 0.70 ± 0.07%, significantly higher than that in WM (0.56 ± 0.05%; $P < 0.05$), although the difference was relatively modest. Together, these results indicate distinct stage-dependent accumulation patterns of HEA and adenosine: HEA was mainly enriched during mycelial growth, whereas adenosine accumulated most prominently in cultivated fruiting bodies.

Differential gene expression and functional interaction network analysis

The volcano plot of differentially expressed genes (DEGs) between AF and AM is shown in Fig. 4A. A total of 1,000 DEGs were identified in this comparison, including 397 upregulated and 603 downregulated genes. In the WF vs WM comparison, 1,080 DEGs were identified, including 495 upregulated and 585 downregulated genes (Fig. 4B). These results indicate that pronounced transcriptional differences existed between fruiting bodies and mycelia under both cultivated and wild conditions.

KEGG functional characteristics of DEGs in AF vs AM

The KEGG pathway enrichment results for DEGs between AF and AM are shown in Fig. 4C. In AF relative to AM, most pathways associated with vegetative growth and basic biosynthesis were mainly enriched among downregulated genes. In particular, downregulated genes were more abundant than upregulated genes in pathways such as ribosome biogenesis in eukaryotes (ko03008), RNA polymerase (ko03020), and cysteine and methionine metabolism (ko00270). In contrast, pathways closely related to developmental differentiation showed stronger enrichment among upregulated genes in AF, especially meiosis–yeast (ko04113) and cell cycle–yeast (ko04111), in which the number of upregulated genes exceeded that of downregulated genes. In addition, starch and sucrose metabolism (ko00500) was also mainly enriched among upregulated genes. Several pathways related to metabolic functional shifts also showed an enrichment trend among upregulated genes in AF, including biosynthesis of various plant secondary metabolites (ko00999), phenylalanine metabolism (ko00360), and degradation of flavonoids (ko00946). In the KEGG annotation system, these pathways mainly reflect changes in gene modules associated with aromatic amino acid metabolism and certain secondary metabolism-related processes.

Overall, the KEGG enrichment pattern of DEGs between AF and AM indicates that the transition from mycelia to fruiting bodies under cultivated conditions involved marked changes in basic biosynthesis, cell cycle regulation, and metabolism-related functional modules.

KEGG functional characteristics of DEGs in WF vs WM

The KEGG pathway enrichment results for DEGs between WF and WM are shown in Fig. 4D. Overall, in most significantly enriched pathways, the number of downregulated genes was greater than or

comparable to that of upregulated genes.

Among pathways related to basic metabolism, purine metabolism (ko00230), glycine, serine and threonine metabolism (ko00260), and valine, leucine and isoleucine degradation (ko00280) were mainly enriched among downregulated genes. Similarly, pathways associated with energy metabolism, such as fatty acid degradation (ko00071) and vitamin B6 metabolism (ko00750), were also dominated by downregulated genes. Among signaling and environmental response-related pathways, the cAMP signaling pathway (ko04024) and MAPK signaling pathway (ko04013) were also mainly enriched among downregulated genes. By contrast, in pathways such as valine, leucine and isoleucine biosynthesis (ko00290) and N-glycan biosynthesis (ko00510), the numbers of upregulated and downregulated genes were relatively comparable. In addition, KEGG pathways annotated as pathways in cancer (ko05200), colorectal cancer (ko05210), and non-small cell lung cancer (ko05223) mainly corresponded in this study to conserved gene modules related to cell cycle regulation, signal transduction, and stress responses. Their enrichment therefore reflects expression differences in these functional modules between wild fruiting bodies and mycelia, rather than disease-related processes.

Overall, the enriched pathways between WF and WM were mainly associated with basic metabolism, energy metabolism, and signal transduction, suggesting broad transcriptional regulation during developmental transition in wild *C. chanhua*.

Protein–protein interaction network analysis

To further explore the potential functional associations of DEGs at the protein level, protein–protein interaction (PPI) networks were constructed for the DEGs identified in AF vs AM and WF vs WM (Fig. 4E–F). In the PPI networks, node size was proportional to node degree, and nodes with higher degrees were generally located in central positions within the network.

In the AF vs AM PPI network (Fig. 4E), TRINITY_DN131_C0_g1, annotated as a putative transcriptional regulator containing MYB-related and bZIP-like domains, was identified as a highly connected hub node and was significantly downregulated in AF relative to AM. Given the important roles of MYB and bZIP domains in transcriptional regulation, the downregulation of this hub gene suggests that certain transcriptional regulatory activities may be reduced during fruiting body formation. This pattern is consistent with the downregulation of transcription- and translation-related pathways observed in the KEGG enrichment analysis. In the WF vs WM PPI network (Fig. 4F), TRINITY_DN80_C0_g1, annotated as a putative transcriptional regulator containing FAR1/GRAS-like domains, occupied a central position in the network and was significantly downregulated in WF. Proteins containing these domains are generally associated with signal transduction and developmental regulation. Therefore, the reduced expression of this hub gene may reflect changes in transcriptional regulatory activity during wild fruiting body development, which is consistent with the overall downregulation of signaling-related pathways, including the cAMP and MAPK signaling pathways.

Integrated transcriptome–metabolome analysis

The sample correlation and chord diagram analysis is shown in Fig. 5A. In the chord diagram, line color and thickness indicate the direction and strength of correlations among samples, with red lines representing positive correlations and green lines representing negative correlations; thicker lines indicate stronger correlations. Correlation analysis showed that cultivated *C. chanhua* samples exhibited higher overall consistency than wild samples. The cultivated fruiting body group (AF) showed high within-group correlations, and the cultivated mycelium group (AM) also showed moderate to high correlations, indicating good reproducibility under artificial cultivation conditions. By contrast, within-group correlations were lower in the wild fruiting body (WF) and wild mycelium (WM) groups, with greater heterogeneity observed among WM samples, suggesting higher inter-individual variation under natural environmental conditions. In addition, cultivated and wild samples were generally negatively correlated, particularly between fruiting body samples, indicating that growth environment had a marked influence on the overall molecular profiles of *C. chanhua* at different developmental stages.

The overlap between differentially accumulated metabolites (DAMs) and differentially expressed genes (DEGs) in the AF vs AM and WF vs WM comparisons is shown in Fig. 5B and 5C, respectively. In the AF vs AM comparison, 48 common differential factors were detected between the transcriptome and metabolome datasets, together with 227 transcriptome-specific DEGs and 15 metabolome-specific DAMs. This result suggests that the differences between cultivated fruiting bodies and mycelia were mainly reflected at the transcriptional level, while a certain degree of transcriptome–metabolome coordination was also present. In the WF vs WM comparison, 36 common differential factors were identified, fewer than those in cultivated samples. The number of transcriptome-specific DEGs increased to 265, whereas the number of metabolome-specific DAMs remained 15, indicating that developmental differentiation between wild fruiting bodies and mycelia was also dominated by transcriptional variation, but with a lower degree of overlap between transcriptomic and metabolic changes.

The integrated analysis of DEGs and DAMs between AF and AM is shown in Fig. 5D. The correlation heatmap showed that most selected DEGs and DAMs were significantly correlated ($|r| > 0.8$, $P < 0.05$) and formed clear clustering patterns. One gene cluster was positively correlated with most metabolites, including lysophospholipids such as LysoPA/LysoPE, the oxidized lipid derivative 9S,10S,11R-trihydroxy-12Z-octadecenoic acid, metabolic intermediates such as L-glutamic acid 5-phosphate and adenylosuccinate, and the triterpenoid-related metabolite ganolucidic acid A. Another gene cluster showed negative correlations with these metabolites. A small number of metabolites, such as 8-propanoylneosolaniol, the cyclic peptide astin I, and several fatty acid derivatives, showed the opposite correlation pattern. These results indicate that, under cultivated conditions, transcriptional changes during the transition from mycelia to fruiting bodies were closely associated with changes in lipid metabolism, amino acid and purine metabolic intermediates, and certain secondary metabolites. This pattern is generally consistent with the metabolic reprogramming revealed by the KEGG enrichment analysis.

The integrated analysis of DEGs and DAMs between WF and WM is shown in Fig. 5E. Compared with cultivated samples, wild samples showed weaker overall transcriptome–metabolome correlations. The heatmap showed that most selected DEGs and DAMs had absolute correlation coefficients below 0.6 and did not form a clear clustering pattern similar to that observed in cultivated samples. Most metabolites, including PA(20:3/18:4), neoacrimarine E, epijasminoside A, AQC2, arginyl-threonine, cis-9,10-epoxystearic acid, momorcharaside A, pokeberrygenin, and several dipeptides and tripeptides, showed relatively weak correlations with genes ($r \approx 0.26–0.56$). A small number of metabolites, including ganoderic acid L, GPCho(18:2/18:2), hexadecanedioic acid mono-L-carnitine ester, mitomycin, oxidized glutathione, and LysoPC(18:3), were negatively correlated with some genes ($r \approx -0.53$ to -0.99). Overall, the correspondence between transcriptional and metabolic changes was weaker in wild samples than in cultivated samples, suggesting a more dispersed molecular regulatory pattern during development under natural conditions.

Taken together, the cultivated fruiting body stage showed stronger transcriptome–metabolome coordination, whereas this coupling was weaker in wild samples. These results indicate that the molecular regulatory characteristics underlying developmental differentiation and bioactive compound accumulation in *C. chanhua* differ markedly between growth environments.

Transcriptome–metabolome correlation network characteristics during developmental differentiation under cultivated and wild conditions

To systematically characterize the molecular associations between cultivated fruiting bodies (AF) and mycelia (AM) of *Cordyceps chanhua*, a correlation network was constructed using differentially expressed genes (DEGs) and differentially accumulated metabolites (DAMs) (Fig. 6A). Overall, the AF vs AM network showed relatively high connectivity, indicating a strong correspondence between transcriptional changes and metabolic alterations during fruiting body formation under cultivated conditions.

At the metabolite level, several DAMs associated with amino acid metabolism, energy metabolism, and membrane lipid remodeling were located in central positions within the network and were significantly correlated with multiple DEGs. L-glutamic acid, D-glutamine, and L-glutamic acid 5-phosphate showed strong correlations with multiple genes, suggesting that glutamate-related metabolism may play an important role in cultivated fruiting body development. Meanwhile, nucleotide-related metabolites, including cGMP, guanosine 3',5'-cyclic monophosphate, and adenylosuccinate, were broadly connected in the network, indicating that energy metabolism and signaling molecule-related processes may be involved in developmental transition under cultivated conditions. Several lipid and lysophospholipid metabolites, such as LysoPE(18:3), LysoPC(18:3), and PE(18:1), were also significantly correlated with multiple DEGs, suggesting dynamic changes in membrane lipid composition during fruiting body formation. At the gene level, several DEGs, including TRINITY_DN2144_c0_g1, TRINITY_DN3505_c0_g1,

and TRINITY_DN5633_c0_g1, showed high connectivity in the network and were positively or negatively correlated with multiple DAMs, indicating that these genes may occupy important positions in the transcriptome–metabolome association network. The coexistence of positive and negative correlations, together with differences in correlation strength, suggests that the transition from mycelia to fruiting bodies under cultivated conditions is a complex process involving coordinated changes in multiple genes and metabolic pathways. Overall, the AF vs AM network revealed strong transcriptome–metabolome coordination during cultivated *C. chanhua* development and provided a basis for identifying key pathways and potential regulatory factors.

To further investigate the molecular association patterns between wild fruiting bodies (WF) and mycelia (WM), a transcriptome–metabolome correlation network was constructed for WF vs WM (Fig. 6B). Compared with the cultivated samples, this network was dominated by negative correlations and showed a relatively dense but more directionally consistent connection pattern, indicating that the transcriptome–metabolome relationships between wild fruiting bodies and mycelia differed markedly from those observed under cultivated conditions.

At the metabolite level, the central metabolites in the network were mainly associated with amino acid metabolism, antioxidant processes, and membrane lipid metabolism. Proline, L-beta-homoproline, and 5'-methylthioadenosine were significantly correlated with multiple DEGs, suggesting that amino acid metabolism and methionine cycle-related processes may be involved in the developmental regulation of wild *C. chanhua*. Oxidized glutathione showed high connectivity in the network, reflecting marked differences in redox-related metabolites between wild fruiting bodies and mycelia. In addition, several phospholipids and lysophospholipids, including PE(16:0/0:0), LysoPC(18:3), GPEtn(18:2/18:2), and GPCho(18:2/18:2), were broadly correlated with multiple DEGs, suggesting that changes in membrane lipid composition may be associated with structural and functional differentiation across developmental stages under wild conditions. At the gene level, several DEGs, including TRINITY_DN5633_c0_g1, TRINITY_DN7510_c0_g1, TRINITY_DN7514_c0_g1, and TRINITY_DN6320_c0_g1, were mainly negatively correlated with multiple DAMs. The fact that individual genes were associated with multiple metabolites suggests a multi-target association pattern between gene expression and metabolite abundance under wild conditions. Unlike the cultivated network, the WF vs WM network did not contain a single dominant hub node with markedly high connectivity, suggesting that developmental differentiation in wild *C. chanhua* may involve a more dispersed and multi-pathway regulatory pattern.

Overall, the WF vs WM network was characterized mainly by negative transcriptome–metabolome associations, with redox-related and lipid metabolism-related metabolites occupying important positions. Compared with cultivated samples, the transcriptome–metabolome coupling in wild samples was relatively weaker, indicating greater complexity in developmental differentiation under natural environmental conditions.

Discussion

Overall molecular differences during developmental differentiation between cultivated and wild *Cordyceps chanhua* and their ecological implications

The multi-omics results of this study showed that cultivated and wild *Cordyceps chanhua* exhibited distinct molecular response patterns during the transition from mycelia to fruiting bodies. Overall, cultivated samples showed higher within-group consistency and clearer stage separation between mycelia and fruiting bodies. In contrast, wild samples showed greater dispersion, with more pronounced inter-individual variation in both transcriptional and metabolic responses. Similar patterns have been reported in other edible fungi. For example, Xiao et al. (2016), based on whole-genome resequencing of wild and cultivated *Lentinula edodes* strains, found that wild populations had higher genetic variation and diversity, whereas cultivated populations showed reduced genetic diversity and greater within-group consistency due to domestication selection. Lee et al. (2020) also reported that wild *L. edodes* strains had significantly higher genetic diversity and population structure dispersion than cultivated strains based on SSR marker analysis. These findings support the general pattern that cultivated materials tend to be more genetically and phenotypically uniform, whereas wild materials exhibit greater variation.

Fruiting body formation in entomopathogenic fungi is highly sensitive to environmental conditions. Previous studies have shown that light, temperature, humidity, nutrient availability, and host or substrate conditions can significantly affect fungal morphogenesis, developmental progression, gene expression programs, and metabolic processes (Kim et al., 2010; Sakamoto, 2018). Therefore, the differences in overall transcriptomic and metabolic profiles between cultivated and wild samples in this study may reflect not only genetic or physiological differences among sample sources, but also the influence of growth environments on developmental regulation in *C. chanhua*. Cultivated systems generally provide relatively stable temperature, humidity, light, and nutrient conditions, which may facilitate a more synchronized molecular response during developmental transition. By contrast, wild *C. chanhua* develops in open and heterogeneous environments, where host status, microhabitat variation, nutrient availability, and environmental stress may jointly contribute to greater molecular heterogeneity.

Studies on *Cordyceps cicadae*, *C. chanhua*, and related cordycipitoid fungi have shown that fruiting body formation is accompanied by stage-specific transcriptional regulation and metabolic remodeling, and that culture conditions or natural habitats can markedly influence metabolic composition and the expression of development-related genes (Lu et al., 2017; Song et al., 2023). From an ecological perspective, the higher consistency observed in cultivated samples and the greater heterogeneity observed in wild samples may reflect differences in developmental regulatory patterns under distinct growth environments. Under cultivated conditions, a stable external environment may favor a more coordinated developmental and metabolic response. Under wild conditions, however, *C. chanhua* may need to dynamically balance developmental progression with environmental adaptation and stress responses. Keller (2019) noted that fungal secondary metabolism is closely associated with development and ecological adaptation, and that the expression of biosynthetic gene clusters is regulated by global transcription factors, epigenetic mechanisms, and environmental stimuli. Bayram and Braus (2012) also emphasized the close coordination between fungal developmental programs and

secondary metabolism, in which biotic and abiotic environmental signals can regulate development and metabolism through Velvet family proteins and the VeA–LaeA regulatory complex.

Taken together, the overall molecular differences between cultivated and wild *C. chanhua* during the mycelium-to-fruiting-body transition reflect both the intrinsic developmental program and the influence of growth environment on fungal developmental and metabolic regulation. The higher consistency observed under cultivated conditions suggests that a stable environment favors a relatively coordinated molecular response, whereas the greater heterogeneity of wild samples indicates that development under natural conditions may be shaped by multiple external factors. These findings provide a basis for understanding quality differences between cultivated and wild *C. chanhua* and their ecological adaptation mechanisms.

Molecular basis of key metabolic pathways and bioactive compound accumulation

This study showed that the transition of *Cordyceps chanhua* from mycelia to fruiting bodies was not merely characterized by changes in individual metabolite levels, but involved coordinated reorganization of multiple metabolic pathways. In cultivated samples, the differential metabolites and enriched pathways at the fruiting body stage were mainly associated with amino acid metabolism, lipid remodeling, and certain secondary metabolic processes, suggesting metabolic adjustments related to tissue development and bioactive compound accumulation under stable cultivation conditions. This pattern is broadly consistent with previous findings in cordycipitoid fungi, in which fruiting body formation is often accompanied by enhanced amino acid metabolism, changes in membrane lipid composition, and activation of secondary metabolism (Lu et al., 2017; He et al., 2023; Sun et al., 2025). Amino acid metabolism can provide nitrogen sources, carbon skeletons, and metabolic precursors for fruiting body development, and may also contribute to the formation of nitrogen-containing bioactive compounds. Xiang Q. et al. (2023) also reported significant enrichment of amino acid metabolism during primordium formation and fruiting body development in edible fungi such as *Hypsizygus marmoreus*, indicating its potential role as a metabolic basis for fungal morphogenesis and secondary metabolism. In parallel, changes in membrane lipid metabolism are generally associated with membrane remodeling, organelle function, and developmental signal transduction. Sakai and Kajiwara (2004) found that phospholipids and cerebrosides changed markedly during mycelial growth and fruiting body differentiation in *Lentinula edodes*, particularly with shifts in fatty acyl composition and increased cerebroside levels at the primordium and fruiting body stages, suggesting that membrane lipid remodeling is an important component of cellular structural adjustment during fruiting body formation.

Compared with cultivated samples, wild samples showed stronger features of environmental response and metabolic homeostasis at the pathway level. The pathways enriched in wild fruiting bodies were more closely related to glutathione metabolism, central carbon metabolism, and redox regulation, suggesting that developmental differentiation in wild *C. chanhua* may depend not only on basic material and energy supply, but also on the maintenance of cellular redox balance and metabolic stability under

natural conditions. He et al. (2019), using HPLC–MS-based metabolomics, reported significant metabolic differences between wild and cultivated *C. chanhua* and their mycelia, which may be influenced by growth environment and host-related factors. Guo et al. (2022) also showed that metabolites associated with glutathione, amino acids, and antioxidant processes were prominent in wild *Cordyceps* species, indicating that complex natural environments may increase the metabolic demand for redox homeostasis and stress responses. In addition, transcriptomic, metabolomic, and multi-omics studies of related cordycipitoid fungi have shown that fruiting body initiation, primordium formation, and maturation are commonly accompanied by coordinated changes in carbohydrate metabolism, fatty acid β-oxidation, the tricarboxylic acid cycle, amino acid metabolism, oxidative phosphorylation, and glutathione metabolism. These metabolic changes can provide energy and precursors for morphogenesis and are associated with the accumulation of bioactive compounds such as cordycepin, adenosine, polysaccharides, and pigments (He et al., 2023; Wang et al., 2023; Zeng et al., 2024). Therefore, the enrichment of central carbon metabolism and glutathione metabolism in wild samples in this study more likely reflects the regulation of developmental progression, energy supply, and redox balance under natural conditions, rather than the specific enhancement of a single class of secondary metabolites.

From the perspective of bioactive compound accumulation, HEA and adenosine showed distinct stage-dependent patterns. HEA was significantly enriched in mycelia and decreased at the fruiting body stage, whereas adenosine was significantly increased in cultivated fruiting bodies and showed a smaller increase in wild fruiting bodies. Zhu et al. (2024) reported that different nitrogen sources and culture conditions significantly affected HEA accumulation in *C. chanhua*, and that amino acid metabolic pathways involving alanine, aspartate, glutamate, and arginine were closely associated with HEA formation. This provides a useful reference for the potential link between HEA enrichment in mycelia and changes in amino acid metabolism observed in the present study. However, the present data do not directly resolve the metabolic flux or key enzymatic steps involved in HEA biosynthesis. Therefore, the causal relationship between HEA accumulation and specific amino acid metabolic nodes requires further validation through targeted metabolomics, isotope tracing, and functional gene analysis.

Adenosine is an important bioactive nucleoside in cordycipitoid fungi and is also a key component of the adenine nucleotide metabolic network, including AMP, ADP, and ATP. Purine metabolism is closely related to energy production, nucleic acid synthesis, and cellular signaling, while the conversion of ATP to ADP, AMP, and adenosine reflects changes in cellular energy status. Adenosine and related purinergic signaling molecules may also participate in the regulation of cell proliferation, differentiation, and development (Singpoonga et al., 2020; Huang et al., 2021). Sun et al. (2025) reported that, during fruiting body formation of *Cordyceps militaris* in liquid culture, amino acid metabolism was mainly enriched during the vegetative growth stage, whereas energy metabolism and purine metabolism were mainly enriched during the reproductive growth stage. This is consistent with the increased adenosine content observed in cultivated fruiting bodies in the present study. Therefore, the significant accumulation of adenosine in cultivated fruiting bodies may be associated with increased energy demand, purine metabolic remodeling, and enhanced development-related metabolic activity during fruiting body

formation. It should be noted, however, that this study mainly revealed associations between adenosine accumulation and developmental stage based on transcriptomic, untargeted metabolomic, and correlation analyses, and cannot directly demonstrate that adenosine accumulation is driven by specific metabolic flux redistribution. Further studies integrating targeted quantification, metabolic flux analysis, and functional validation of key enzymes are needed to clarify the regulatory mechanisms underlying HEA and adenosine accumulation.

In summary, the reconstruction of key metabolic pathways during developmental differentiation in *C. chanhua* showed clear source-dependent features. Cultivated samples were characterized by metabolic adjustments related to fruiting body development, amino acid metabolism, membrane lipid remodeling, and bioactive compound accumulation, whereas wild samples were more strongly associated with central carbon metabolism, glutathione metabolism, and redox homeostasis. The differential accumulation of HEA and adenosine across developmental stages further indicates that nucleoside formation is closely related to developmental stage and cultivation environment. These findings help explain the metabolic basis of quality differences between cultivated and wild *C. chanhua* and provide a foundation for future improvement of high-quality *C. chanhua* production through cultivation optimization, key pathway analysis, and functional gene validation.

Transcriptome–metabolome coordination network and its implications for cultivation optimization

The transcriptome–metabolome association network further revealed distinct patterns of molecular coordination between cultivated and wild *Cordyceps chanhua* during developmental differentiation. Compared with wild samples, cultivated samples showed a more compact association structure between differentially expressed genes and differentially accumulated metabolites. The correlations were more concentrated, suggesting a higher degree of consistency between transcriptional changes and metabolic remodeling during the transition from mycelia to fruiting bodies under controlled cultivation conditions. Previous studies on cordycipitoid fungi have shown that fruiting body formation is usually accompanied by stage-specific gene expression and metabolic reprogramming, and that pathways related to development, energy supply, and bioactive compound biosynthesis often change coordinately at specific developmental stages (Lu et al., 2017; He et al., 2023; Thananusak et al., 2023). Therefore, the relatively compact transcriptome–metabolome network observed in cultivated samples may reflect stronger coordination between development-related gene expression and metabolic responses under stable cultivation conditions.

From a network perspective, the stronger gene–metabolite correlations in cultivated samples should not be interpreted simply as direct regulatory relationships. Rather, they more likely indicate that multiple developmental and metabolic modules change coordinately at the same developmental stage. Integrated transcriptomic analysis of *Cordyceps militaris* has shown clear stage-specific expression differences between mycelia and fruiting bodies, with related genes mainly involved in the cell cycle,

amino acid metabolism, carbohydrate metabolism, and lipid metabolism. Fruiting body development is also accompanied by changes in polysaccharide metabolism, glycerolipid metabolism, and glycerophospholipid biosynthesis, which are associated with the accumulation of bioactive compounds such as cordycepin (Thananusak et al., 2023). Similarly, integrated transcriptomic and metabolomic analysis of primordium initiation in Chinese cordyceps showed that genes and metabolites related to starch and sucrose metabolism, fructose and mannose metabolism, fatty acid degradation, and glycerophospholipid metabolism changed synchronously during primordium germination, suggesting that carbohydrate metabolism and fatty acid β-oxidation may provide energy and metabolic substrates for fruiting body initiation (He et al., 2023). In addition, transcriptome–metabolome network analysis of cordycepin synthesis in *C. militaris* indicated that purine metabolism, the TCA cycle, the pentose phosphate pathway, amino acid metabolism, and ABC transporters may jointly participate in bioactive compound formation (Wang et al., 2023). Consistent with these findings, the compact network structure observed in cultivated *C. chanhua* suggests coordinated responses among multiple functional modules, including developmental regulation, energy metabolism, membrane lipid remodeling, and bioactive compound-related metabolism.

In contrast, the transcriptome–metabolome network of wild samples showed a more dispersed association pattern without prominent hub nodes, indicating that gene expression changes and metabolite accumulation during development under natural conditions did not exhibit a highly centralized correspondence. Previous studies have reported significant differences in metabolic composition between wild and cultivated *C. chanhua*, which may be associated with host background, habitat conditions, and environmental stress (He et al., 2019). Therefore, the more dispersed network structure in wild samples may be related to the combined effects of multiple environmental factors under natural conditions. It should be noted that a dispersed network does not necessarily indicate lower regulatory efficiency; rather, it may reflect greater inter-individual variation and a more complex regulatory background in wild *C. chanhua*. Because the present network analysis was based primarily on correlations, it cannot establish causal regulatory relationships between specific genes and metabolite accumulation. The candidate hub nodes identified here therefore require further functional validation.

These network differences provide useful implications for cultivation optimization. The stronger transcriptome–metabolome coupling in cultivated samples suggests that cultivation conditions may be optimized to improve the coordination between development-related pathways and the accumulation of target metabolites. Future cultivation strategies should move beyond empirical approaches such as increasing nutrient supply or extending cultivation time, and should instead integrate multi-omics information to focus on key modules associated with fruiting body development and bioactive compound accumulation, including developmental regulation, amino acid metabolism, carbohydrate metabolism, membrane lipid remodeling, purine metabolism, and secondary metabolism. Previous studies on cordycipitoid fungi have shown that these pathways are closely associated with fruiting body development and functional metabolite accumulation (Lu et al., 2017; He et al., 2023; Thananusak et al., 2023; Wang et al., 2023). Accordingly, future studies combining environmental factor gradient experiments, targeted metabolite quantification, metabolic flux analysis, and functional gene validation

will help identify key regulatory steps affecting fruiting body formation and the stable accumulation of bioactive compounds in *C. chanhua*.

In summary, the differences in transcriptome–metabolome coordination between cultivated and wild *C. chanhua* reflect distinct organizational patterns of developmental regulation and metabolic responses under different growth environments. Under cultivated conditions, *C. chanhua* tends to form a more compact and coordinated transcriptome–metabolome response network, which facilitates the identification of candidate modules related to fruiting body formation and target metabolite accumulation. Under wild conditions, the more dispersed network structure suggests that developmental and metabolic responses may be shaped by multiple environmental factors. These findings provide additional evidence for understanding the molecular basis of developmental differentiation and bioactive compound formation in *C. chanhua*, and offer a useful reference for cultivation optimization and quality control based on multi-omics network analysis.

Conclusion

Integrated transcriptomic and untargeted metabolomic analyses showed that wild and cultivated *Cordyceps chanhua* exhibited distinct transcriptome–metabolome response patterns during the transition from mycelia to fruiting bodies. Cultivated samples showed more compact gene–metabolite associations, whereas wild samples displayed a more dispersed metabolic regulatory pattern. In addition, HEA and adenosine accumulated differentially across developmental stages, suggesting stage-dependent formation of bioactive nucleosides. This study provides multi-omics evidence for differences in developmental differentiation, metabolic reprogramming, and nucleoside accumulation between wild and cultivated *C. chanhua*, thereby improving our understanding of the molecular basis of quality formation in this fungus. The results suggest that cultivation optimization should focus on key modules such as amino acid metabolism, lipid remodeling, purine metabolism, and secondary metabolism to improve the stability and controllability of target bioactive compound accumulation. Future studies integrating targeted metabolite quantification, metabolic flux analysis, functional validation of key genes, and cultivation parameter optimization will further clarify the mechanisms underlying bioactive compound formation and provide scientific support for high-quality raw material production, quality evaluation, and functional product development of *C. chanhua*.

Abbreviations

AF Artificial cultivated fruiting bodies of *Cordyceps chanhua*

AM Artificial cultivated mycelia of *Cordyceps chanhua*

WF Wild fruiting bodies of *Cordyceps chanhua*

WM Wild mycelia of *Cordyceps chanhua*

HEA N6-(2-hydroxyethyl)adenosine

LC–MS Liquid chromatography–mass spectrometry

UPLC Ultra-high-performance liquid chromatography

ESI Electrospray ionization

QC Quality control

TIC Total ion chromatogram

BPC Base peak chromatogram

PCA Principal component analysis

DEGs Differentially expressed genes

DAMs Differentially accumulated metabolites

KEGG Kyoto Encyclopedia of Genes and Genomes

PPI Protein–protein interaction

FMN Flavin mononucleotide

cGMP Guanosine 3',5'-cyclic monophosphate

FC Fold change

PCC Pearson correlation coefficient

P value Probability value

Declarations

Acknowledgements

The authors gratefully acknowledge the Lianyungang Academy of Agricultural Sciences for providing research resources and support.

Authors' contributions

WJ, XL, and XT conceived the idea, acquired funding, designed the experiments, and wrote and submitted the manuscript. WJ, JG, WS, and WC participated in resource acquisition and wrote the first draft. WJ and LH performed the experiments. WJ and FL conducted data investigation and analysis. All authors read and approved the final manuscript.

Funding

This work was supported by the 2025 Jiangsu Edible Mushroom Industry Cluster Project (Liannongfa [2025] No. 248), the 2024 Lianyungang Key Research and Development Plan Project (SF2404), the Lianyungang Municipal Financial Special Fund (QNJJ2506), the 2025 Lianyungang Characteristic Agricultural Industry Development Project (Liannongfa [2025] No. 287).

Data availability

The metabolomic datasets used in this study are available from the corresponding author upon reasonable request.

Ethics approval and consent to participate

Not applicable.

Consent for publication

Not applicable.

Competing interests

The authors declare that they have no competing interests.

Author details

[1] Lianyungang Academy of Agricultural Sciences, Lianyungang 222000, China.

[2] Jiangsu Key Laboratory for Horticultural Crop Genetic Improvement, Institute of Vegetable Crops, Jiangsu Academy of Agricultural Sciences, Nanjing 210014, China.

[3] Jiangsu Key Laboratory of Marine Bioresources and Environment, Jiangsu Ocean University, 59 Cangwu Road, Haizhou District, Lianyungang 222005, China.

References

1. Bayram, Ö., & Braus, G. H. (2012). Coordination of secondary metabolism and development in fungi: The velvet family of regulatory proteins. *FEMS Microbiology Reviews*, *36*(1), 1–24. https://doi.org/10.1111/j.1574-6976.2011.00285.x
2. Cai, R., Xiao, Y., Xing, J., Yu, K., Li, X., & Chai, Y. (2024). Establishment of a genetic transformation system for cordycipitoid fungus *Cordyceps chanhua*. *Frontiers in Microbiology*, *15*, 1333793. https://doi.org/10.3389/fmicb.2024.1333793
3. Cai, R. H., Li, X. L., Liu, Y. G., Fang, M., Liu, Z., & Chai, Y. Q. (2025). Identification and expression analysis of microRNAs in spores and fruiting bodies of *Cordyceps chanhua* [in Chinese].

Mycosystema, *44*(5), 53–64. https://doi.org/10.13346/j.mycosystema.240329

4. Cao, M., Wu, J., Zhu, X., Jia, Z., Zhou, Y., Yu, L., Hu, C., Gao, Y., & Chen, Z. (2024). Tissue distribution of metabolites in *Cordyceps cicadae* determined by DESI-MSI analysis. *Analytical and Bioanalytical Chemistry*, *416*, 1883–1906. https://doi.org/10.1007/s00216-024-05188-x
5. Di, F., Zhang, J., Cheng, W., Li, L., Li, M., & Wang, C. (2023). Paecilomyces cicadae: A systematic overview of the biological activities and potential mechanisms of its active metabolites. *Food and Agricultural Immunology*, *34*(1). https://doi.org/10.1080/09540105.2023.2243059
6. Ding, Z. Z. (2021). Preliminary comparative transcriptome analysis of *Thelephora ganbajun* at different developmental stages [Master's thesis, Yunnan University]. https://doi.org/10.27456/d.cnki.gyndu.2021.001187
7. Dong, M., Zhao, C., Huang, Y., Zheng, K., Bao, G., Hu, F., Peng, F., Chen, M., Li, Z., & Lu, R. (2024). Metabolites analysis and new bioactive compounds from the medicine food homology product of *Cordyceps chanhua* on artificial media. *Journal of Pharmaceutical and Biomedical Analysis*, *237*, 115749. https://doi.org/10.1016/j.jpba.2023.115749
8. Ghirardo, A., Fochi, V., Lange, B., Witting, M., Schnitzler, J. P., Perotto, S., & Balestrini, R. (2020). Metabolomic adjustments in the orchid mycorrhizal fungus *Tulasnella calospora* during symbiosis with *Serapias vomeracea*. *New Phytologist*, *228*(6), 1939–1952. https://doi.org/10.1111/nph.16812
9. Guo, S., Lin, M., Xie, D., Zhang, W., Zhang, M., Zhou, L., Li, S., & Hu, H. (2022). Comparative metabolic profiling of wild *Cordyceps* species and their substituents by liquid chromatography-tandem mass spectrometry. *Frontiers in Pharmacology*, *13*, 1036589. https://doi.org/10.3389/fphar.2022.1036589
10. He, L., Xie, F., Zhou, G., Chen, Z. H., Wang, J. Y., & Wang, C. G. (2023). Transcriptome and metabonomics combined analysis revealed the energy supply mechanism involved in fruiting body initiation in Chinese cordyceps. *Scientific Reports*, *13*, 9500. https://doi.org/10.1038/s41598-023-36261-7
11. He, Y., Zhang, W., Peng, F., Lu, R., Zhou, H., Bao, G., Wang, B., Huang, B., Li, Z., & Hu, F. (2019). Metabolomic variation in wild and cultured cordyceps and mycelia of *Isaria cicadae*. *Biomedical Chromatography*, *33*, e4478. https://doi.org/10.1002/bmc.4478
12. Hsu, J. H., Chen, Y. Y., Lin, T. W., Chiang, I. T., Chiang, L. H., & Chen, C. C. (2026). Comparative chemical profiles of fruiting bodies and mycelia of *Cordyceps cicadae* and *Ophiocordyceps sobolifera*, and immunometabolic modulation by liquid-fermented mycelia. *Fitoterapia*, *188*, 107028. https://doi.org/10.1016/j.fitote.2025.107028
13. Huang, Z., Xie, N., Illes, P., Di Virgilio, F., Ulrich, H., Semyanov, A., Verkhratsky, A., Sperlagh, B., Yu, S. G., Huang, C., & Tang, Y. (2021). From purines to purinergic signalling: Molecular functions and human diseases. *Signal Transduction and Targeted Therapy*, *6*, 162. https://doi.org/10.1038/s41392-021-00553-z
14. Ji, W., Su, W. Y., Wang, Y. P., Liu, X. M., Ren, L. K., Yang, Z. W., Zhou, Z. Y., & Chen, K. L. (2024). Breeding of elite strains of *Cordyceps chanhua* [in Chinese]. *Journal of Anhui Agricultural University*, *51*(4), 697–705. https://doi.org/10.13610/j.cnki.1672-352x.20240830.020

15. Ji, W., Wang, Y., Liu, X., Su, W., Ren, L., Wang, H., & Chen, K. (2025). Genetic diversity analysis of wild *Cordyceps chanhua* resources from major production areas in China. *Diversity*, *17*(2), 85. https://doi.org/10.3390/d17020085
16. Kanehisa, M., & Goto, S. (2000). KEGG: Kyoto encyclopedia of genes and genomes. *Nucleic Acids Research*, *28*(1), 27–30. https://doi.org/10.1093/nar/28.1.27
17. Kanehisa, M., Furumichi, M., Sato, Y., Matsuura, Y., & Ishiguro-Watanabe, M. (2025). KEGG: Biological systems database as a model of the real world. *Nucleic Acids Research*, *53*(D1), D672–D677. https://doi.org/10.1093/nar/gkae909
18. Keller, N. P. (2019). Fungal secondary metabolism: Regulation, function and drug discovery. *Nature Reviews Microbiology*, *17*, 167–180. https://doi.org/10.1038/s41579-018-0121-1
19. Kim, S. Y., Shrestha, B., Sung, G. H., Han, S. K., & Sung, J. M. (2010). Optimum conditions for artificial fruiting body formation of *Cordyceps cardinalis*. *Mycobiology*, *38*(2), 133–136. https://doi.org/10.4489/MYCO.2010.38.2.133
20. Lee, H. Y., Moon, S., Ro, H. S., Chung, J. W., & Ryu, H. (2020). Analysis of genetic diversity and population structure of wild strains and cultivars using genomic SSR markers in *Lentinula edodes*. *Mycobiology*, *48*(2), 115–121. https://doi.org/10.1080/12298093.2020.1727401
21. Lee, S. C., Alaali, L., Kwon, H., Rigi, M., & Eberhart, C. G. (2022). Cordycepin (3'-deoxyadenosine) suppresses heat shock protein 90 function and targets tumor growth in an adenosine deaminase-dependent manner. *Cancers*, *14*(13), 3122. https://doi.org/10.3390/cancers14133122
22. Li, C. R., Wang, Y. Q., Cheng, W. M., Chen, Z. A., Hywel-Jones, N., & Li, Z. Z. (2021). Review on research progress and prospects of cicada flower, *Isaria cicadae* (Ascomycetes). *International Journal of Medicinal Mushrooms*, *23*(4), 81–91. https://doi.org/10.1615/IntJMedMushrooms.2021038085
23. Li, S. P., Yang, F. Q., & Tsim, K. W. K. (2006). Quality control of *Cordyceps sinensis*, a valued traditional Chinese medicine. *Journal of Pharmaceutical and Biomedical Analysis*, *41*(5), 1571–1584. https://doi.org/10.1016/j.jpba.2006.01.046
24. Lu, Y., Luo, F., Cen, K., Xiao, G., Yin, Y., Li, C., Li, Z., Zhan, S., Zhang, H., & Wang, C. (2017). Omics data reveal the unusual asexual-fruiting nature and secondary metabolic potentials of the medicinal fungus *Cordyceps cicadae*. *Bmc Genomics*, *18*, 668. https://doi.org/10.1186/s12864-017-4060-4
25. Nxumalo, W., Elateeq, A. A., & Sun, Y. (2020). Can *Cordyceps cicadae* be used as an alternative to *Cordyceps militaris* and *Cordyceps sinensis*? A review. *Journal of Ethnopharmacology*, *257*, 112879. https://doi.org/10.1016/j.jep.2020.112879
26. Sakai, H., & Kajiwara, S. (2004). Membrane lipid profile of an edible basidiomycete *Lentinula edodes* during growth and cell differentiation. *Lipids*, *39*, 67–73. https://doi.org/10.1007/s11745-004-1203-9
27. Sakamoto, Y. (2018). Influences of environmental factors on fruiting body induction, development and maturation in mushroom-forming fungi. *Fungal Biology Reviews*, *32*(4), 236–248. https://doi.org/10.1016/j.fbr.2018.02.003

28. Siddiqui, J. K., Baskin, E., Liu, M., Cantemir-Stone, C. Z., Zhang, B., Bonneville, R., McElroy, J. P., Coombes, K. R., & Mathé, E. A. (2018). IntLIM: Integration using linear models of metabolomics and gene expression data. *Bmc Bioinformatics*, *19*, 81. https://doi.org/10.1186/s12859-018-2085-6
29. Singpoonga, N., Rittiron, R., Seang-on, B., Chaiprasart, P., & Bantadjan, Y. (2020). Determination of adenosine and cordycepin concentrations in *Cordyceps militaris* fruiting bodies using near infrared spectroscopy. *ACS Omega*, *5*, 27235–27244. https://doi.org/10.1021/acsomega.0c03403
30. Song, L., Shrivastava, N., Gai, Y., Li, D., Cai, W., Shen, Y., Lin, F. C., Liu, J., & Wang, H. (2023). Role of the blue light receptor gene *Icwc-1* in mycelium growth and fruiting body formation of *Isaria cicadae*. *Frontiers in Microbiology*, *13*, 1038034. https://doi.org/10.3389/fmicb.2022.1038034
31. Sun, Y., He, B., Cao, X., Li, Z., Xu, L., Li, Y., & Guo, S. (2025). Metabolomics analysis reveals the formation mechanism of *Cordyceps militaris* fruiting bodies in liquid culture. *Food Chemistry*, *495*, 146651. https://doi.org/10.1016/j.foodchem.2025.146651
32. Thananusak, R., Laoteng, K., Raethong, N., Koffas, M., & Vongsangnak, W. (2023). Dissecting metabolic regulation in mycelial growth and fruiting body developmental stages of *Cordyceps militaris* through integrative transcriptome analysis. *Biotechnology and Bioprocess Engineering*, *28*, 406–418. https://doi.org/10.1007/s12257-022-0207-5
33. Wan, J., Zhu, Y., Jiang, X., Wang, F., Zhou, Z., Wang, J., Liu, C., Wei, Y., & Ouyang, Z. (2023). Immunomodulation of RAW264.7 cells by CP80-1, a polysaccharide of *Cordyceps cicadae*, via Dectin-1/Syk/NF-κB signaling pathway. *Food and Agricultural Immunology*, *34*(1). https://doi.org/10.1080/09540105.2023.2231172
34. Wang, X., Li, Y., Li, X., Sun, L., Feng, Y., Sa, F., Ge, Y., Yang, S., Liu, Y., Li, W., & Cheng, X. (2023). Transcriptome and metabolome profiling unveils the mechanisms of naphthalene acetic acid in promoting cordycepin synthesis in *Cordyceps militaris*. *Frontiers in Nutrition*, *10*, 1104446. https://doi.org/10.3389/fnut.2023.1104446
35. Wang, Y., Zeng, T., Li, H., Wang, Y., Wang, J., & Yuan, H. (2023). Structural characterization and hypoglycemic function of polysaccharides from *Cordyceps cicadae*. *Molecules*, *28*(2), 526. https://doi.org/10.3390/molecules28020526
36. Xiang, Q., Arshad, M., Li, Y., Zhang, H., Gu, Y., Yu, X., Zhao, K., Ma, M., Zhang, L., He, M., & Chen, Q. (2023). Transcriptomic profiling revealed important roles of amino acid metabolism in fruiting body formation at different ripening times in *Hypsizygus marmoreus*. *Frontiers in Microbiology*, *14*, 1169881. https://doi.org/10.3389/fmicb.2023.1169881
37. Xiao, Y., Cheng, X., Liu, J., Li, C., Nong, W., Bian, Y., Cheung, M. K., & Kwan, H. S. (2016). Population genomic analysis uncovers environmental stress-driven selection and adaptation of *Lentinula edodes* population in China. *Scientific Reports*, *6*, 36789. https://doi.org/10.1038/srep36789
38. Yang, T., Guo, M., Yang, H., Guo, S., & Dong, C. (2016). The blue-light receptor CmWC-1 mediates fruit body development and secondary metabolism in *Cordyceps militaris*. *Applied Microbiology and Biotechnology*, *100*, 743–755. https://doi.org/10.1007/s00253-015-7047-6

39. Yin, Y., Yu, G., Chen, Y., Jiang, S., Wang, M., Jin, Y., Lan, X., Liang, Y., & Sun, H. (2012). Genome-wide transcriptome and proteome analysis on different developmental stages of *Cordyceps militaris*. *Plos One*, *7*(12), e51853. https://doi.org/10.1371/journal.pone.0051853
40. Zeng, Z., Zou, Y., Cai, W., Lin, F. C., & Wang, H. (2024). Roles of CcDFR and CcOMT9 in the cyanidin biosynthesis and development of *Cordyceps cicadae*. *Frontiers in Microbiology*, *15*, 1353710. https://doi.org/10.3389/fmicb.2024.1353710
41. Zheng, R., Xu, Q., Wang, Y. W., Zhong, Y. F., & Zhu, R. (2024). *Cordyceps cicadae* polysaccharides attenuate diabetic nephropathy via the miR-30a-3p/TRIM16 axis. *Journal of Diabetes Investigation*, *15*, 300–314. https://doi.org/10.1111/jdi.14116
42. Zhu, K., Ruan, H., Wu, T., Zhang, H., Han, W., & Shen, Q. (2024). Exploiting the roles of nitrogen sources for HEA increment in *Cordyceps cicadae*. *Frontiers in Microbiology*, *15*, 1384027. https://doi.org/10.3389/fmicb.2024.1384027
43. Zhu, Q., Shi, N., Zhang, Y., Peng, F., Yang, G., & Huang, B. (2023). Complete genome sequence of a novel victorivirus infecting cicada flower (*Cordyceps chanhua*). *Archives of Virology*, *168*, 4. https://doi.org/10.1007/s00705-022-05640-2

Figures

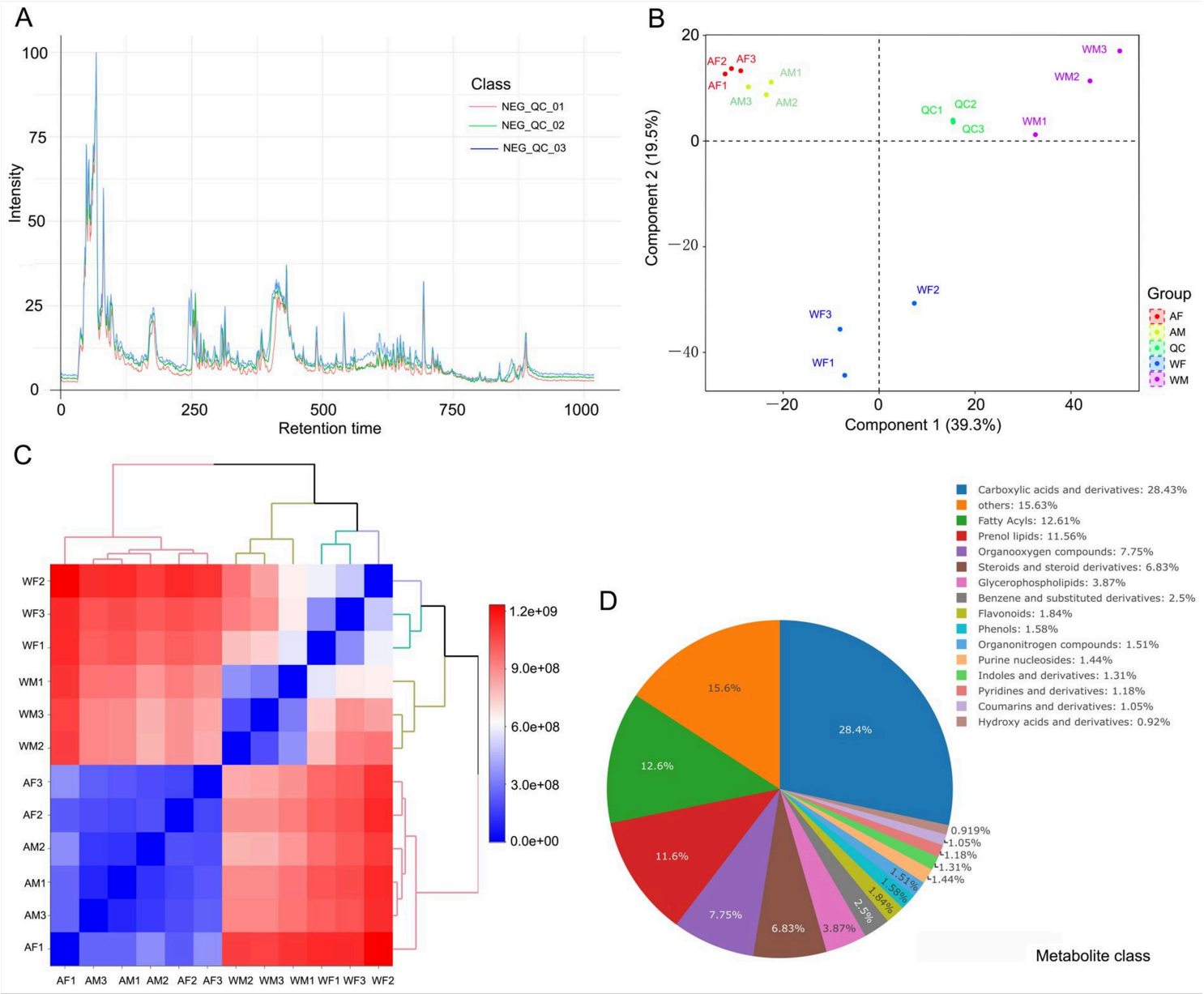


Figure 1

Metabolomic quality control and multivariate statistical analysis. **(A)** Base peak chromatograms (BPCs) of QC samples in positive ion mode. **(B)** Principal component analysis (PCA) score plot used to evaluate overall data quality and reproducibility. **(C)** Sample distance heatmap based on Euclidean distance. **(D)** Chemical classification of the identified metabolites.

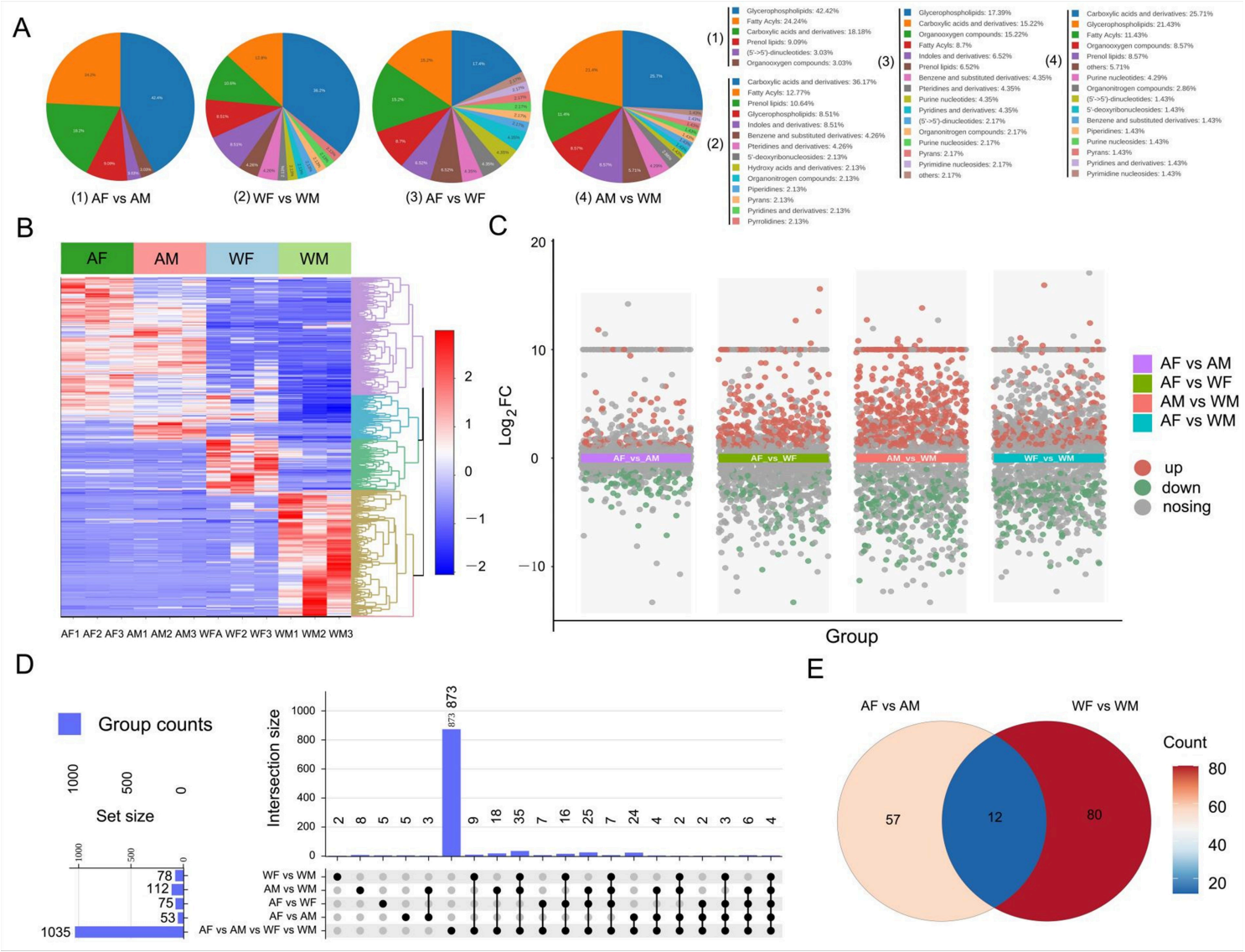


Figure 2

Screening and characterization of differential metabolites. **(A)** Pie charts showing the chemical classification of differential metabolites in each comparison group. **(B)** Hierarchical clustering heatmap based on the relative abundances of differential metabolites. **(C)** Volcano plots of differential metabolites. **(D)**UpSet plot showing the shared and specific differential metabolites among comparison groups. **(E)** Venn diagram showing the shared and unique differential metabolites between selected comparison groups.

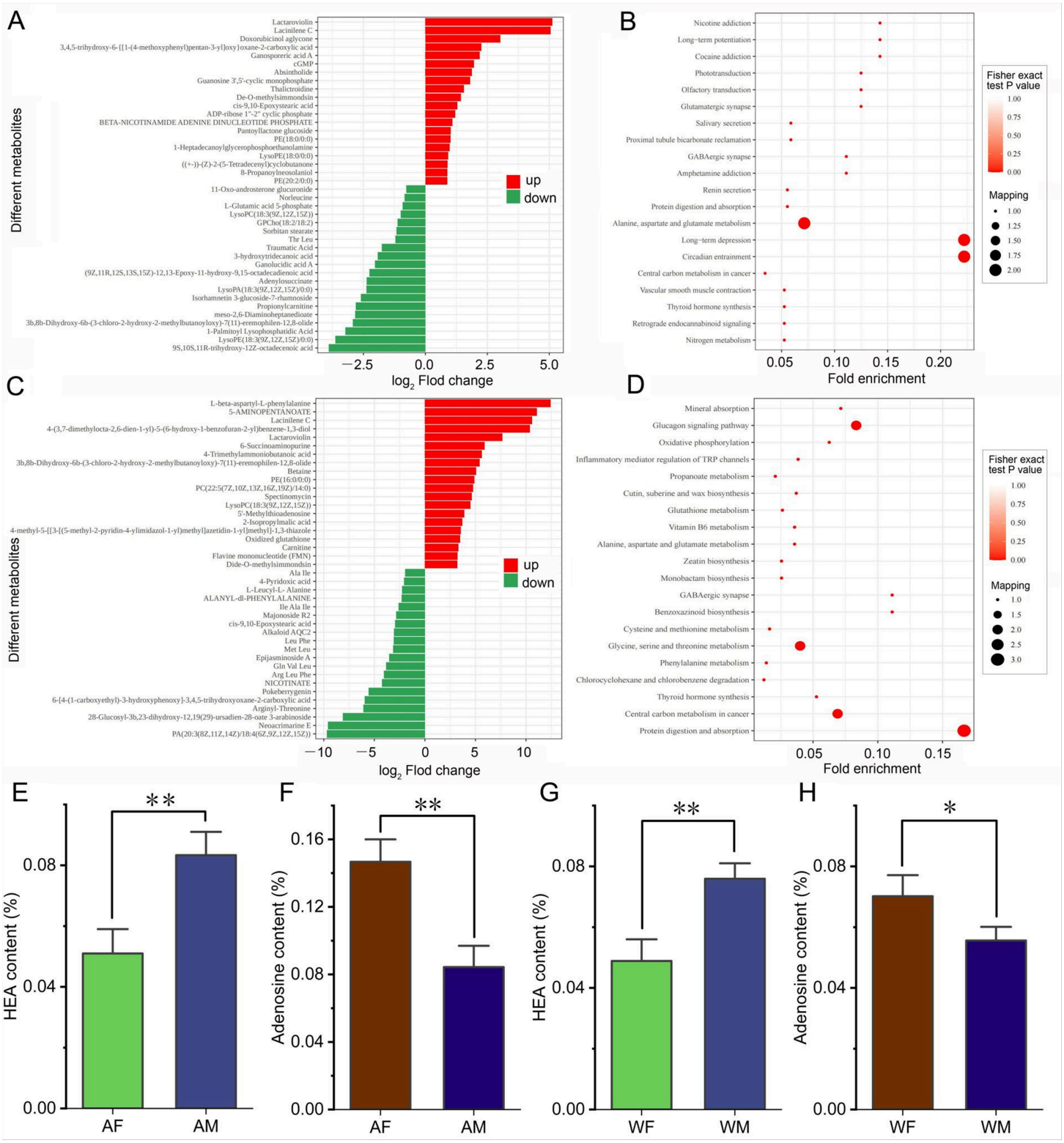


Figure 3

Differential metabolites and KEGG pathway enrichment analysis. (A) Bar plot showing the $\log_2$ fold changes of differential metabolites between AF and AM. **(B)** KEGG pathway enrichment bubble plot of differential metabolites between AF and AM. **(C)** Bar plot showing the $\log_2$ fold changes of differential metabolites between WF and WM. **(D)** KEGG pathway enrichment bubble plot of differential metabolites between WF and WM. **(E)** Difference in HEA content between AF and AM. **(F)** Difference in adenosine

content between AF and AM. **(G)** Difference in HEA content between WF and WM. **(H)** Difference in adenosine content between WF and WM.

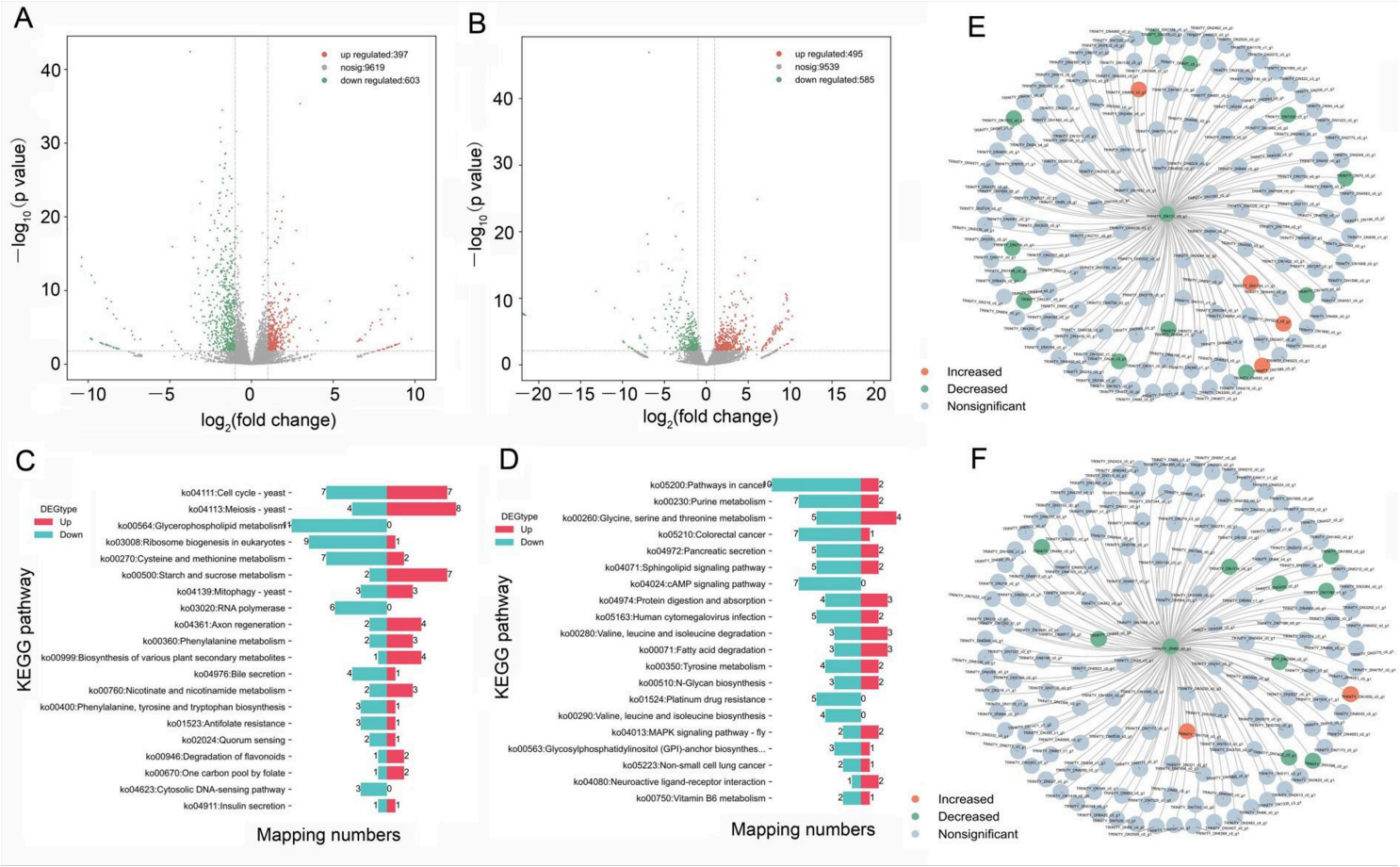


Figure 4

Differential gene expression patterns and functional interaction networks between artificial and wild *Cordyceps chanhua*. **(A)** Volcano plot of differentially expressed genes (DEGs) between AF and AM. **(B)** Volcano plot of differentially expressed genes (DEGs) between WF and WM. **(C)** KEGG pathway enrichment analysis of DEGs between AF and AM (butterfly plot). **(D)** KEGG pathway enrichment analysis of DEGs between WF and WM (butterfly plot). **(E)** Protein–protein interaction (PPI) network of DEGs between AF and AM. **(F)** Protein–protein interaction (PPI) network of DEGs between WF and WM.

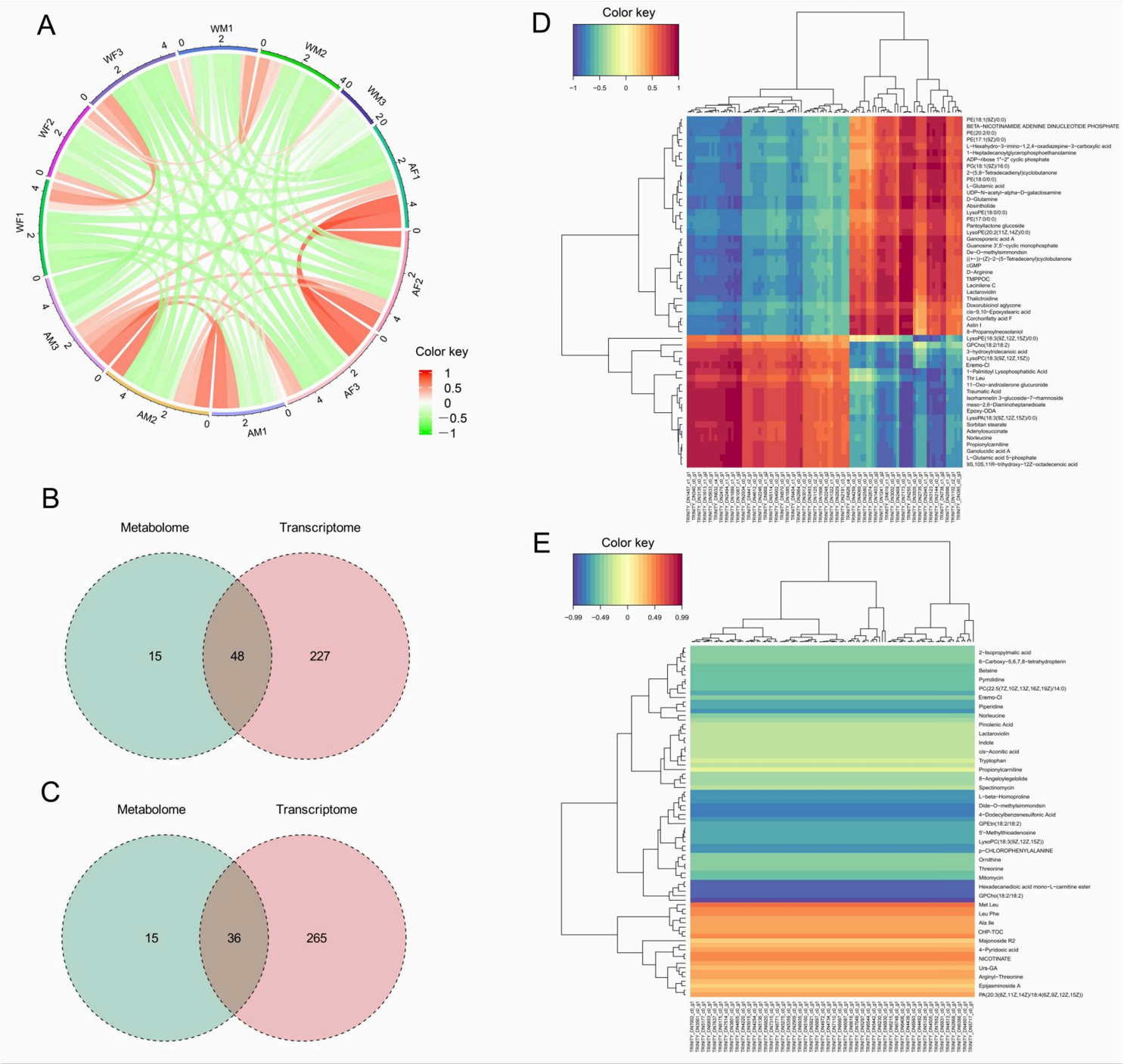


Figure 5

Sample correlation and integrated analysis of differentially expressed genes and metabolites. **(A)** Chord diagram showing correlations among samples. **(B)** Venn diagram showing the overlap between differentially expressed genes and differentially accumulated metabolites in the AF vs AM comparison. **(C)** Venn diagram showing the overlap between differentially expressed genes and differentially accumulated metabolites in the WF vs WM comparison. **(D)** Correlation heatmap of differentially expressed genes and differentially accumulated metabolites in the AF vs AM comparison. **(E)** Correlation heatmap of differentially expressed genes and differentially accumulated metabolites in the WF vs WM comparison.

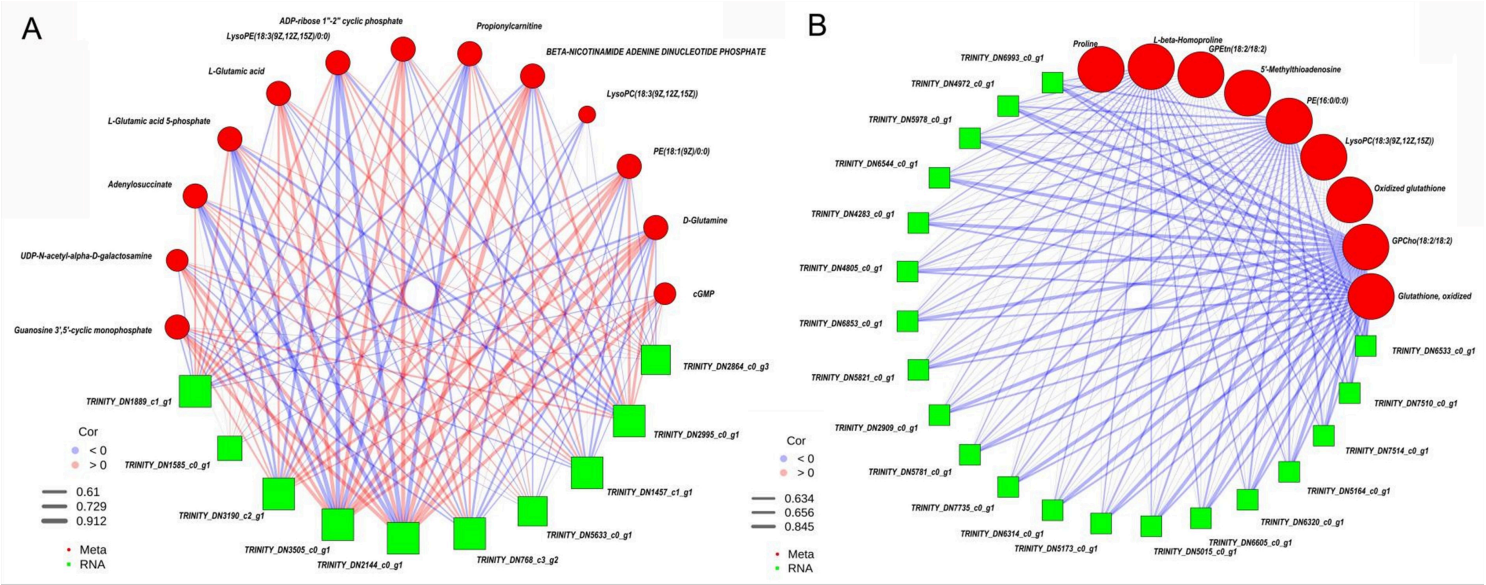


Figure 6

Integrated transcriptome–metabolome correlation networks between fruiting bodies and mycelia of *Cordyceps chanhua* under artificial and wild conditions. **(A)**Transcriptome–metabolome correlation network between artificial fruiting bodies (AF) and mycelia (AM). **(B)** Transcriptome–metabolome correlation network between wild fruiting bodies (WF) and mycelia (WM).

Supplementary Files

This is a list of supplementary files associated with this preprint. Click to download.

- floatimage1.jpeg